OPTICAL FINE-STRUCTURE OF A MENISCUS IN ANALYTICAL ULTRACENTRIFUGATION IN RELATION TO MOLECULAR-WEIGHT DETERMINATIONS USING THE ARCHIBALD PRINCIPLE

RODES TRAUTMAN*

The Rockefeller Institute for Medical Research, New York, N.Y. (U.S.A.)

The centripetal and centrifugal limits of the solution column in an analytical ultracentrifuge cell are positions that it is important to know accurately for two reasons. In the first place the starting level of a moving boundary can be used in the determination of sedimentation rates[1], and secondly, the limits through which there is no transport of solute can be used in the determination of molecular weight[2]. During a study of this later case, which may be called an application of the ARCHIBALD principle, it became apparent that the level through which no solute crossed into the air space above the solution did not coincide with the center of the optical registration of the meniscus. Investigation was then made of the meniscus pattern as a function of camera focus and the angle of incidence of the light on the cell. It developed that a meniscus is responsible for very complex diffraction and interference phenomena. In fact, conditions are easily obtainable in which two separate central shadows are visible.

There is some suggestion in the literature on the application of the ARCHIBALD principle that there may be difficulties in the location of the limits of the solution column. Thus CHENG[3] has called attention to the dependence of the calculated molecular weight on choice of meniscus position, which for bovine serum albumin he calculates to be about 10 %/0.1 mm in the cell when early pictures are used. Comparing the width of a photodensitometer tracing of the fine-structure of a meniscus with the width of a sharp desoxyribonucleic acid boundary as a function of speed, he concludes that the decrease in meniscus width with speed is more than accounted for by change in vibration or precision of the rotor. The balance he attributes to change in surface-tension effects. Inspection of microdensitometer tracings of absorption-optical registrations in the literature revealed that the center of the shadow (high transmission) has been chosen as the meniscus[4]. However, some tracings have shown complex biphasic patterns[5]. BROWN[6] discusses foreshortening of the full cell due to the steep gradients deflecting light into the bottom. But GINSBURG, APPEL AND SCHACHMAN[7] interpret the thickening of the bottom meniscus as being due to a packed gel and as being an indication of the amount of denatured solute and high sedimenta-

* Part of this work was carried out while the author was a research collaborator in the Medical Department, Brookhaven National Laboratory, Upton, L.I., New York. Present address of author is U. S. Dept. of Agriculture, Plum Island Animal Disease Laboratory, Greenport, L.I., New York.

References p. 431.

tion-rate contamination present in the original solution. Further, these same workers have also called attention to a broader meniscus at low speed due to vibration. KEGELES, KLAINER AND SALEM[8] describe foreshortening of the empty cell image due to light entering the cell at an angle. But the last two groups assume that both the air-solution and solution-dense immiscible-fluid menisci shadows are correct.

It is the purpose of this paper to present (a) studies using the ARCHIBALD principle which pertain to the location of the true top of the solution column, (b) studies of factors contributing to the optical fine-structure of a meniscus, and (c) a method for determining the location of an interface to within $\pm$ 0.005 mm in the cell. This study was facilitated by providing the back plate of the camera of a standard Model E Spinco ultracentrifuge* with a clear glass insert so that the actual image to be photographed could be observed. Although this is a desirable improvement, it is not essential for the full use of the suggestions made here for the improved precision of schlieren-pattern analysis.

EXPERIMENTAL

Ultracentrifuge modifications

Alteration of the schlieren-diaphragm mount to permit thumb-screw cross motion has been described[1]. The further modification of a Spinco Model E ultracentrifuge to incorporate a removable glass in the focal plane of the camera will now be given. After removing the right-side cover plate, the back plate of the camera mechanism in which the plate holder travels is accessible. This was removed for the milling of a 2–3/4″ × 3″ hole. A holder, accurately held in position by two pins, was fashioned to be inserted in this opening so that the outside surface of a 1/16″-thick clear glass was located at the plane corresponding to the emulsion of the photographic plate. When the camera was used in the ordinary manner, the glass holder was removed and replaced by an appropriate light-tight cover. To facilitate measurements of the image relative to the camera, a 0.008″-diameter vertical stainless steel wire was fastened in the camera aperture plate (2″ × 2″). This wire was not affected by the glass holder, and permanently cast a vertical shadow in the reference band transmitted by the reference edges 90° from the cell holes in the Spinco Analytical AN-D rotor; alternatively the outer reference hole in the counterbalance was used (see Fig. 2). The cylindrical lens axis is normally the primary reference direction in the Spinco schlieren-optical system. In this laboratory, the camera wire was used as reference and the cylindrical lens was rotated slightly so that the image lines on the calibration scale as an object in the rotor, were parallel to it. Observations of images on the clear glass insert were made with a 20-mm scale-contact ocular with 0.1 mm divisions**. The standard Spinco field change of a swing-out mirror to replace the half-surface mirror was made. It should be noted that the Spinco interference-optics-viewer assembly does not accomplish exactly the same purpose as the camera focus-insert glass. The viewer does not accurately focus in the plane of the ground glass, or of the photographic plate, not does it permit measurements to be made. Furthermore, a back-surface mirror is used in the swing-out assembly. The usual ground-glass viewing screen is essentially useless for studying fine-structure of diffraction patterns. Metallographic plates were used for photographing the effects displayed in this paper.

Various cells were assembled from modified standard Spinco parts as indicated in Fig. 1. When it was desired to have the baseline on the plate simultaneously with the protein pattern, a double-sector centerpiece cell was chosen[10], Fig. 1(c). The special channel mask (a) was made out of 2024-T4 aluminum alloy 0.032″ thick, 0.618″ in diameter. It fits on top of the upper disc holder (b) and is oriented to allow transmission of light from the solution side only. The counterbalance is increased by 0.4 g when the mask is used before or after a normal experiment in the double-sector cell. In order to make a highly reflecting surface perpendicular to the axis of rotation, a plain quartz disc, normally used as a window of a centrifuge cell, was coated with rhodium***. The coated side of this disc could be oriented in any one of the four possible positions in the cell. One position is shown in (f). The coating does not cover the entire surface, so an air–water meniscus, for example, can be made near the bottom of the cell. Then the transmitted meniscus pattern can

* Spinco Division, Beckman Instruments, Inc., Palo Alto, California.
** Bausch and Lomb Optical Co., Rochester, New York, Cat. No. 81-34-97-20.
*** Evaporated Metal Films, Inc., Ithaca, N. Y.

References p. 431.

be studied for various positions of the light source (k). Because of the length of the light source, all points cannot be on the optical axis. Hence a mask (i) with slot (j) will give a reflection (h) from the mirror quartz. This arrangement allows measurement of the distance by which the light source

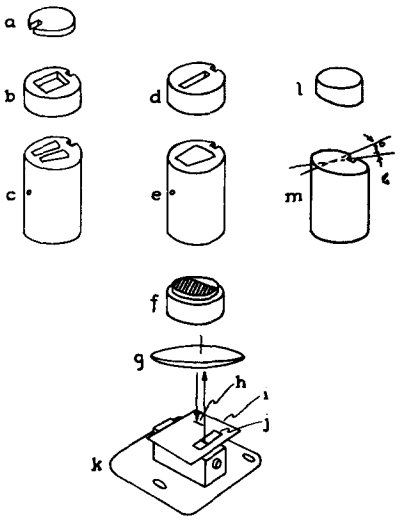

Fig. 1. Arrangement of cells for special optical applications. Only the parts which are different from the standard components are illustrated. a. Cover for one channel of double-sector centerpiece c, which rests inside screw ring on enlarged aperture disc-holder b. d. Narrow aperture mask dischoIder for very wide (7°) centerpiece e. f. Mirror lower quartz disc causing reflection of light back through lower collimating lens g to h on a white card i with slot j. k. Light-source mount of ultracentrifuge. l. Prism quartz disc in inverted position for use with prism centerpiece m for non-sedimentation experiments.

is off-axis. Three 1/2″-long spacer washers were used to extend the light source legs so that the light source slit was at the focal point of the lower collimating lens when the chamber was closed and under vacuum. This was determined by the position of the sharpest reflected image. Prior to obtaining the reflecting quartz disc, a 12-mm epoxy double-sector centerpiece in which the center partition (e) had been removed, was half-filled with mercury. A small amount of water could be used on top of the mercury, again to give simultaneously a transmitted air–water meniscus and a strong reflected image. Extreme caution should be exercised when using mercury. In particular, use of a metal centerpiece with gaskets should be avoided, and a speed of 17,000 r.p.m. should not be exceeded. In the experiments here, the lowest speed setting of 12,590 r.p.m. was not exceeded with the mercury-mirror cell. No such limitation is imposed on the quartz-mirror cell.

For special study of optical effects, and in particular to determine the effect of non-parallel quartz windows, a 1° prismatic cell was made. The epoxy centerpiece shown at (m) had its upper face milled at a 1° angle so that the thickness at the keyway—the most radial position—is thinner than at the opposite side. In order to effect a seal, a 1° wedge quartz was used in a plain disc holder (l). This 1° quartz prism oriented in this manner deflects the light from the *air space* in a radial direction and hence the shadow of the schlieren diaphragm is above that caused by the light passing through the reference hole (vacuum). On the other hand, light through the *water space* is deflected centripetally by the water prism at low speed and radially a greater amount by the quartz prism. At 60,000 r.p.m. the compression gradient in water compensates the water prism and there is no relative displacement on the schlieren diaphragm of the light-source image of rays passing through the air space or the water space. It should be noted that this prismatic centerpiece is only for instrumentation studies of the optical phenomena involved.

In order to know what plane in the cell was imaged on the photographic plate or insert glass, the focal position of the camera objective lens along its optical track for various planes was determined. A hair was clamped between each quartz and the face of both the 3-mm and 12-mm centerpieces. With the chamber open and a ground glass diffusing screen placed on top of the lower collimating lens, the position of sharpest focus of each hair was determined. The position with and without the cylindrical lens showed only 0.02″ difference and was certainly more easily located without the cylindrical lens. The 12-mm cell air thickness corresponds to 0.84″ of camera-lens movement.

For comparison, a two-dimensional microcomparator reading to 0.01 mm on the plate was used (basic magnification of the schlieren optical system is 2.18). The equipment and the pertinent mathematical relations have been described[1]. Extensive use was made of the duplex printing calculator *Tetractys** which facilitated calculations necessary for the ARCHIBALD plots of Figs. 3 and 7.

* Olivetti Corporation of America, New York, N.Y.

References p. 431.

Materials

Armour crystalline ribonuclease (RNAse), formula weight 13,700, lot no. 381–059 was used[9] in acetate buffer, pH 5.5 and ionic strength 0.1. Urea was added to this system to 6 M concentration for some experiments. The nature of this solute–solvent system is immaterial for the purposes of this paper. This complex mixture is designed to exaggerate anomalies, if they exist, in the application of the ARCHIBALD principle.

Dow Corning Silicone Fluid No. 555, suggested by GINSBURG, APPEL AND SCHACHMAN[7], was used to form a meniscus radial to the air–water meniscus. Benzene and bromobenzene with H_2O or D_2O were also used to form menisci of various surface-tension and index of refraction combinations. The water-contact angle was altered in one experiment by siliconizing the quartz discs with General Electric Co. Dri Film.

ARCHIBALD *principle*

The ARCHIBALD principle[2] makes no reference to speed; hence it should be valid in high-speed velocity ultracentrifugation as well as low-speed equilibrium ultracentrifugation. Prior to complete separation of the boundary region from the meniscus, this principle, as presented by KEGELES, KLAINER AND SALEM[8], states that at the upper geometrical limit of the solution r_a the concentration gradient will adjust itself as the concentration falls so that

$$M\,(1-\bar{v}\varrho)\,\omega^2 r_a - \left(\frac{\partial\mu}{\partial r}\right)_{T,P,r_a} = 0 \tag{1}$$

where M, $\bar{v}$ and μ are the (anhydrous) molecular weight, partial specific volume and molar chemical potential, respectively, of the solute component, ω, T and P are the constant angular velocity, absolute temperature and pressure at r_a, and R is the gas constant. This can be rearranged to

$$M_{\text{app}}\,(1-\bar{v}\varrho) \equiv \frac{RT\,(\partial c/\partial r)_{r_a}}{\omega^2 r_a c_a} = \frac{M\,(1-\bar{v}\varrho)}{1+(\partial \ln y/\partial \ln c)} \tag{2}$$

where M_{app} is an apparent molecular weight calculated as though the activity coefficient y were unity. It should be noted that the concentration can be expressed in any units, and further, if index of refraction or optical density are used for the concentration determination, the appropriate value of y can be chosen to allow for deviations from a first degree relationship to a mass concentration scale.

Not only can the concentration c_a be determined directly from the schlieren pattern but also the concentration c at any level between r_a and r_p, a point in the plateau solution, from

$$c = c^0 - \int_{r_a}^{r_p} \left(\frac{r}{r_a}\right)^2 \frac{\partial c}{\partial r}\,\mathrm{d}r + \int_{r_a}^{r} \frac{\partial c}{\partial r}\,\mathrm{d}r \tag{3}$$

Hence it is possible to calculate from schlieren patterns a quantity δ at each level in the cell defined as

$$\delta \equiv \frac{RT\,\partial \Delta n/\partial r}{\omega^2 r \Delta n} \tag{4}$$

where Δn is the increment to the index of refraction of the solution contributed by the solute component. The inclusion of RT/ω^2 in the calculation of δ is to allow direct comparison of experiments at different speeds and/or temperatures and to convert to molecular weight units, for at $r = r_a$, $\delta = \delta_a$ where

$$\delta_a = M_{\text{app}}\,(1-\bar{v}\varrho) \tag{5}$$

References p. 431.

ARCHIBALD proposed[2], in effect, that δ be plotted as a function of r for each photograph. In the event δ_a was independent of time, all the curves would intersect, thereby determining both r_a and δ_a. Since a foreknowledge of r_a is required in order to evaluate equation (3), it appears that this method of analyzing the schlieren patterns precludes determination of r_a. However, in principle, successive approximations can be used, first choosing an r_a, calculating δ in the neighborhood of r_a for several photographs, then from an apparent common intersection correcting the value of r_a and recalculating δ.

RESULTS

Location of r_a *by use of the* ARCHIBALD *principle*

In Fig. 2 are shown the stages of separation of a ribonuclease boundary from the meniscus at 59,780 r.p.m. The S rate is 0.7 Svedbergs in this urea solvent of density d_4^{20} 1.1014. Pictures after 256 min allow the initial concentration c° to be measured,

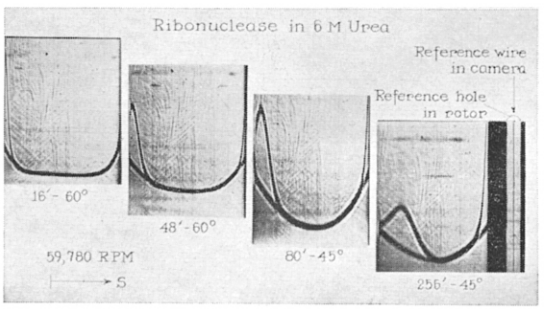

Fig. 2. Schlieren patterns during formation of a sedimenting boundary. Phaseplate schlieren optics with a double-sector centerpiece cell; the time in minutes from 2/3 of the operating speed is given at the left under each frame, while the schlieren diaphragm angle is given at the right. Concentration is 9 mg/ml.

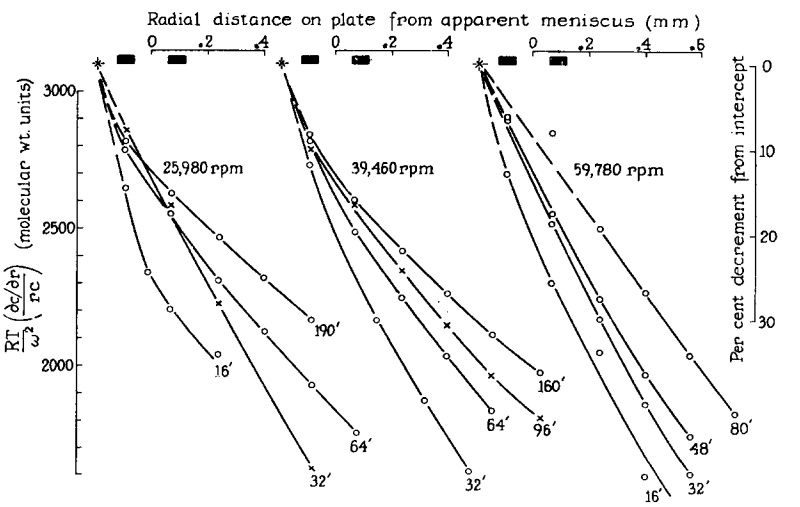

Fig. 3. ARCHIBALD plots for early times in the sedimentation of ribonuclease in 6 M urea. Three separate experiments are shown and denoted by the speed. The time in minutes of each frame is indicated at the lower right by each curve. The solid blocks represent the edges of the central shadow of the meniscus. The asterisk represents the best value of δ_a for these data. 0.1 M acetate buffer, pH 5.5, before addition of crystalline urea to 6 M, 9 mg/ml ribonuclease.

References p. 431.

since the concentration gradient at the meniscus has dropped to zero. In Fig. 3, right-hand side, is shown the δ *vs.* r plot for the patterns of Fig. 2. The solid rectangles represent the darker edges on either side of the central shadow cast by the meniscus. These curves have been calculated by assuming, quite arbitrarily, that r_a is given by the center of the left-hand darker edge of the meniscus pattern. Usually the meniscus is considered to be the center of the shadow indicated by the zero in the scale above these curves. These data are for the region within a few tenths of a millimeter of the meniscus and represent the first step in the study of its fine-structure. Thus Fig. 3 reveals that the apparent position of the meniscus in this experiment does not correspond to the common intersection of the curves, indicated by an asterisk. Recalculation of eqn. (3) shows that the change of r_a by 0.1 mm in the lower limit of the integrals has no appreciable effect on the location of the common intersection of these curves. However, the change of 0.1 mm in the choice of r_a for any one curve has a pronounced effect on the value of δ_a determined thereby—of the order of 5–10%.

The same calculations made for experiments at 39,460 r.p.m. and 25,980 r.p.m. are shown in the center and left portions of Fig. 3, respectively. At 160 min the pattern at 39,460 was similar to the 48-min frame of Fig. 1. But at 25,980 r.p.m. at 190 min, the pattern was still of the type indicated by the 16-min frame of Fig. 1. The curves of Fig. 3 show the same general shape even though the schlieren pattern may rise or fall proceeding radially from the meniscus. They also show marked curvature but, more important for this study, they reveal that at all three speeds, the true top of the solution did not correspond to the optical registration of the meniscus, if it be assumed that M_{app} is a constant.

Variation of optical registration from a meniscus

Bearing in mind the observations of others mentioned in the introduction, the cylindrical lens was removed and the meniscus pattern studied with the ocular on the focal-plane glass insert to see if the position could vary enough to account for the 0.1 to 0.2 mm discrepancy of Fig. 3. Vibration at low speed was of the order of $\pm$ 0.03 mm. It was present even with accurately balanced cells and appeared to increase with the age of the drive. Occasional precession of the rotor was also observed. This was as much as $\pm$ 0.1 mm on the plate but had a period of the order of 1 hour. Detection was made by measuring the position of the camera vertical-wire shadow relative to the reference edges, as in Fig. 2, 4th frame. Quite unexpected was the appearance of another "meniscus" as the camera was focused about 3 mm lower in the cell. This new meniscus appeared toward the center of rotation, a fact that would qualitatively account for the discrepancy indicated in Fig. 2.

In order to make clear the type of optical anomaly that is being considered in this paper, and prior to a detailed description of experiments without the phaseplate schlieren diaphragm[1] or cylindrical lens, an extreme case showing the complexity in the meniscus region is presented in Fig. 4. At the right-hand side is shown a (ribonuclease) protein solution at a time during the formation of a boundary. The light source has been moved toward the front of the ultracentrifuge so that the parallel light enters the cell at a 1° angle from the air side as indicated schematically by the arrow. This is a single-sector cell giving two "menisci". Note that the solution deflection extends only to the outer of these shadows (proceeding from the bottom of the cell toward the top), for a negative deflection can be seen interior to the two

References p. 431.

"menisci". At the left of Fig. 4 the air–water interface at a lower speed, 12,590 r.p.m., is shown for both positions of the light source off-axis. The deflection of the light between the "menisci" changes sign and hence cannot be due to the gradient of the index of refraction passing from air to water. Note also the additional fine vertical bands.

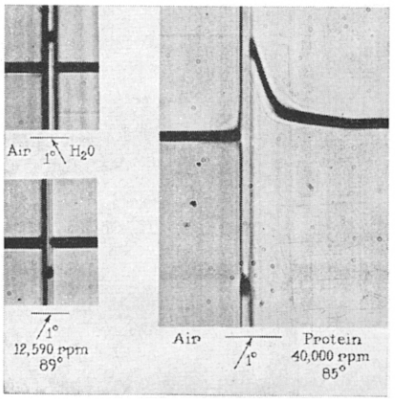

Fig. 4. Optical complexity of the meniscus region. Centrifugation is to the right in a single-sector centerpiece cell with phaseplate schlieren optics. Left-hand photographs are for air–water interface at 12,590 r.p.n. at 89° schlieren diaphragm angle for 1° oblique illumination entering the cell along the direction indicated by the arrow. Right-hand photograph is for air–protein during the separation of the boundary from the meniscus.

Conditions not influencing meniscus fine-structure

Several possible factors contributing to the complex fine-structure of the meniscus region displayed in Fig. 4 could be eliminated at the outset. Thus the effect of the side walls of the cell—the centerpiece side itself—was checked by using a 2° mask as the upper quartz-disc holder and a 7° centerpiece, Figs. 1(d) and (e). There is no difference between the pattern for this arrangement and that for the obverse, having a 2° centerpiece with a 7° mask. The effect of diverging light was tested by raising the light source and/or lowering the lower collimating lens by opening the rotor chamber. The results indicate that the double-meniscus effect is not due to an error in the location of the light source at the focal distance of the lower collimating lens. Both the 12-mm and 3-mm cells were used simultaneously, filled to slightly different levels, to determine the effect of cell height. The separation of the double-meniscus pattern was less for the thinner cell. Thus fine-structure is not specific for the 12-mm cell, but the depth of the optical object must be taken into account. It was further found that the meniscus pattern was unaffected by the position of a point light source moved perpendicular to the radius being photographed. That is, a line light source in the position for schlieren optics, parallel to the meniscus could be used. The effect of the cylindrical lens and the phaseplate half-wave coating could then be tested directly, since the cylindrical lens is focused along the length of the light source at the phaseplate. Thus in Fig. 4, the vertical lines of the fine-structure are independent of the position along the light source or schlieren diaphragm.

Effect of off-axis illumination and camera focus

The experiments to be described revealed factors which influenced the complex meniscus pattern and indicated what part of the region, extending over a millimeter or so on the plate, contained information about the geometrical top of the solution column.

References p. 431.

A composite of many of the effects photographed without the cylindrical lens or phaseplate is shown in Fig. 5. The upper edge of the centerpiece is termed the "front face" of the cell, "O". The lower edge, at a distance "a", is termed the "back face" The fractions indicate intermediate positions of focus in the air space. Consider the second row of pictures. These are for the air–water meniscus at 52,640 r.p.m. and for the camera focused at 5a/12. At the left is the double-meniscus picture for light entering from the air side at 1/2° from the normal, then for normal illumination indicated by the vertical arrow, and for 1/2° deviation the opposite side of the normal. Further to the right is the pattern for 1° angle of incidence, and at the same time the top pattern in the vertical column (b) showing the effect of speed from 52,640 to 12,590 and finally to 3,000 r.p.m. The width and separation of the main double shadow increases with decreasing speed. At the 12,590 r.p.m. level, in the third row from the top are shown on either side the effect of changing focus—to the left, focusing on

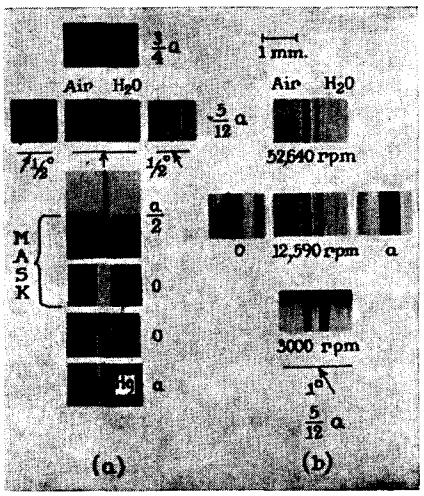

Fig. 5. Effect of focus and oblique illumination on the optical fine structure of the meniscus region. "a" refers to focus on the lower face of the centerpiece in the air space and "o" refers to the upper face, nearest the camera. The arrows and angles indicate direction and angle of incidence of light on the cell. Line at upper right shows 1 mm on the plate. Column (a) shows effect of focus for on-axis illumination. Column (b), the effect of speed for off-axis illumination. See text for explanation of Mask- and Hg-patterns.

the front face, and to the right, focusing on the back face. Note that the pattern becomes very broad and asymmetrical. This corresponds to accentuating either the left or the right one of the two main shadows.

Returning to the left top row of Fig. 5, the narrowest meniscus trace is obtained for the focus at 3a/4 with the light source on axis. Following this vertical column (a) down, skipping some of the pictures, the central shadow gets broader and the flanking bands spread wider apart as the focus is shifted toward the front face of the cell: 3a/4, 5a/12, and 0, the second row from the bottom. In the bottom row is a pattern of a mercury–water interface, showing diffraction-like bands in the water space only since no light can pass through the mercury.

In the third row from the bottom in column (a), white, corresponding to light, appears in the position where the central shadow lies in the pattern below. This was obtained by masking the light-source images with an opaque strip from the air and water space in the schlieren diaphragm plane. This means that the central shadow is due not only to light deflected out of the optical system by an infinite gradient—which would be infinitely thin anyway—but also to an interference phenomenon.

References p. 431.

Not too clearly visible in this photographs, in the third row from the bottom, are the flanking bands on either side. Thus the light which passes through the main light-source image at the schlieren-diaphragm plane does not contribute to these bands. The effect of the mask blocking out the main light-source image at the schlieren diaphragm can be compared simultaneously with the effect of no mask, by using the cylindrical lens to focus along the light-source image, part of which is obscured by the mask. The result is shown in the center of column (a), the tallest photograph labeled a/2. The prism-centerpiece cell was used at top speed, thus both the air and the water light-source images superimposed at the schlieren diaphragm plane, and were blanked out simultaneously along half their length by a single very narrow, 1 mm opaque strip. This photograph shows that the fine-structure of the meniscus pattern without the mask is the same for the prismatic cell as for one with parallel windows. Comparing the "no mask" and "mask" portions, it shows further that the central shadow splits into two interference fringes still flanked by the diffraction bands. The former are called interference fringes, for if the light from either half plane on either side of the mask is also blanked out, the fringes are destroyed, leaving only light. Also, if the phaseplate is oriented at 0° so that the light on one side passes through the coated portion, the character and spacing of the interference fringes is altered. It is to be expected that there will be light throughout the schlieren-diaphragm plane where there are deflections due to index of refraction gradients in the cell. It was, however, unexpected to find finite deflections on both sides of the undeflected light-source image from the "infinite gradient" of the meniscus itself. This was observed with the light source on the axis. When it was off-axis, a major deflection appeared on one side only, but reversed with the movement of the light source to the other side of the optical axis, as has already been shown in Fig. 4.

Subclassification of meniscus optical fine-structure

From the foregoing experiments it can be concluded that there are two basically different phenomena giving rise to the normal optical fine-structure of a meniscus, without any obstruction in the schlieren-diaphragm plane. The first gives rise to a relatively broad band called here the "central shadow". The second gives rise to two sets of ordered finer diffraction-like bands on either side of the central shadow, called here the "flanking fringes". The central shadow is involved in an interference-type effect, for its further sub-structure can be revealed by appropriate aperture stops. The resulting bands are referred to as "interference bands".

Effect of the nature of the fluids forming the interface

Various combinations of immiscible fluids were studied in order to determine which portion of the interface is responsible for each of the two effects mentioned above. The light source was placed accurately on the optical axis, by use of the mirror cell, to simplify the central shadow, as suggested by Fig. 5.

The results of one series of experiments are shown in Fig. 6. At the top is a schematic side-view of the cell with air, benzene, water, and bromobenzene, forming the immiscible phases. The direction of the contact angle is shown for each interface. Two other properties must also be considered. One is the refraction index of the fluid, for this changes the level of focus. For example, the horizontal dotted lines indicate the plane which is in focus in the various fluids, if the center of the air space is in

References p. 431.

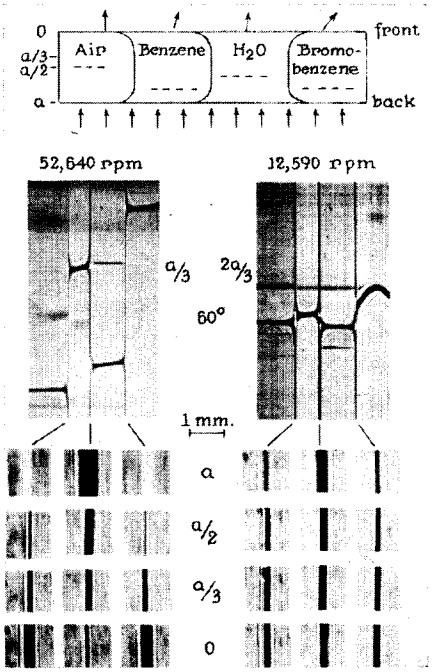

Fig. 6. Effect of physical properties of the fluids forming the interface on the central shadow of the meniscus region for on-axis illumination. Upper drawing: schematic arrangement of cell. Centrifugation is to the right. Arrows below indicate direction of incident light, arrows above indicate qualitatively the deflection caused by the compression gradient. Center photographs: phaseplate schlieren optics at 60° for two speeds. 52,640 r.p.m. on left and 12,590 r.p.m. on right. In each, the left-hand vertical black line is the air–benzene interface, the center black line is the benzene–water interface, and the right-hand black line is the water–bromobenzene interface. Lower sets of 12 photographs each: magnified views of the interfaces without phaseplate or cylindrical lens, enlarged to the scale indicated by the 1-mm mark in the center. Four levels of focus are shown.

focus. The second effect is due to the refractive-index gradient caused by the compression gradient in each of the various fluids. This gives a deflection indicated qualitatively by the arrows at the top of the figure, and quantitatively by the vertical displacement of the cylindrical lens phaseplate-schlieren patterns shown in the center of the figure. Two speeds are shown, since the compression refractive gradient depends upon the square of the speed.

The photographs at the bottom in Fig. 6 were taken without the cylindrical lens or schlieren diaphragm, and correspond in vertical columns to the interface marked with a line to the cylindrical lens patterns. Four planes of focus are shown: at the back face in the air space, a; the center of the air space, a/2; the center of the water-space, approximately a/3 in air; and the front face, o. The light is normal to the cell when it enters. These sets of pictures are to be compared in columns to show the effect of camera focus on a given interface. At a given focus, they are to be compared as a function of speed for a given interface. Finally, in any row, at either speed, the effect of different fluids can be compared. Two general statements can be made about these patterns. (a) The central shadow is quite variable. Depending on the system, it can either increase or decrease in width with speed, probably owing to the change in refractive-index gradient with speed more than to the change in contact angle. (b) The flanking fringes on either side of the central shadow appear independent of the nature of the fluids forming the interface, or the speed at a given plane of focus. Their spacing and sharpness are inversely related—the spacing increasing for all interfaces as the plane of focus is moved toward the camera.

Experimental problem and proposed solution

As far as the application of the ARCHIBALD principle is concerned, the problem is

References p. 431.

to determine which part of the fine-structure of the complex meniscus registration is a precise determinant of the true top of the solution column. Being unaware of a theoretical solution to this optics problem, I interpret the experimental results to mean that the central shadow is caused by the contacts of the interface with the front and back windows, and the flanking fringes to be a diffraction effect from the flat portion of the interface itself between the windows. No specific band, light or shadow, interference or diffraction, corresponds in position to the flat portion of the interface—the "infinite index of refraction gradient". For practical purposes, it can be assumed that the bisector between any pair of corresponding flanking fringes is the position of the interface. This will not lie at the center of the central shadow if the light source if off-axis by even 1 mm. However, it is worth-while to adjust the light source on the axis by means of the image reflected from the mirror cell in any case so that (a) the solution-gradient pattern will be visible close to the interface, and (b) the center of the central shadow can be used if vibration or photographic conditions obscure the flanking fringes. With double-sector-cell experiments, the additional meniscus from the solvent side may confuse the interpretation of the solution-side meniscus pattern. Hence, at the conclusion of an experiment, it is advisable to insert a channel mask, as in Fig. 1(a), to blank out the solvent sector, reaccelerate to the speed used in the experiment, and photograph the solution meniscus. Since the width of a flanking fringe is only a few hundredths of a millimeter on the plate, the bisector can be located to within $\pm$ 0.005 mm in the cell.

Indirect check using the ARCHIBALD *principle*

After adjusting the optics in this manner, ribonuclease, without urea, was studied and yielded the result shown in Fig. 7. Although the solvent was not the same, the type of plot is directly comparable to Fig. 3. It shows that the common intersection does now coincide with the bisector of the flanking fringes. The dotted arrows indicate a position 0.2 mm more radial than the common intersection. The spread of the curves here is to be compared with that at the corresponding level in Fig. 3, which is located

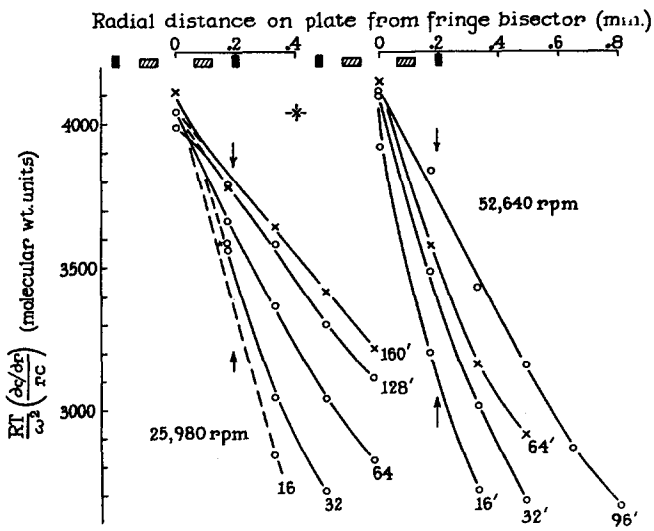

Fig. 7. ARCHIBALD plot for early times in the sedimentation of ribonuclease without urea, light source aligned. Two separate speeds are shown. The time in min of each frame is indicated at the lower right by each curve. The shaded blocks represent the edges of the central shadow as in Fig. 3. The solid blocks represent one pair of the flanking fringes. The vertical arrows indicate the level 0.18 mm from the common intersection corresponding to the level of the zero in Fig. 3. The asterisk represents the best value of δ_a for these data. 0.1 *M* acetate buffer, pH 5.5, 9 mg/ml ribonuclease.

References p. 431.

at the center of the (not aligned) central shadow. The value $\delta_a = 4{,}040$, together with $\bar{v} = 0.709$ and $\varrho = 1.003$, gives $M_{app} = 14{,}000$. The formula weight is 13,700. It was not possible to see the flanking fringes on the plates of the experiments in Fig. 2, and thus obtain directly the true meniscus r_a for comparison with the common intersection.

DISCUSSION

Fig. 8 is a schematic drawing indicating the optical problem of an interface deep in optical path length compared with the viewing plane, which has its conjugate image interior to this object. Here an equivalent form[11,12] of the schlieren-optical system has been chosen to simplify the problem: C is the cell with two media with refraction indices n′ and n″, L is the lens imaging planes P' and P'' at P. The upper part (Fig. 8a) shows the effect of the location of the plane of focus P′—P″ on the apparent separation of the shadows of the intersection of the meniscus with the front and back quartz windows. The fact that the camera cannot be focused on both contacts simultaneously accounts for most of the behavior of the central shadow—for example that it appears displaced, or double, if the light source is off the optical axis, and that if double, the separation is less for a thin cell than for a thick one. The effect of the actual contact angle is indeed complex, but of lesser importance than the optical discontinuity at the intersection of the interface with the window. Thus, above about 4,000 r.p.m., the double central shadow for off-axis illumination was the same whether siliconized or normal quartz discs were used with an air–water interface. However, below 4,000 r.p.m. the width and separation showed hysteresis and other variability usually encountered in contact-angle measurements[13].

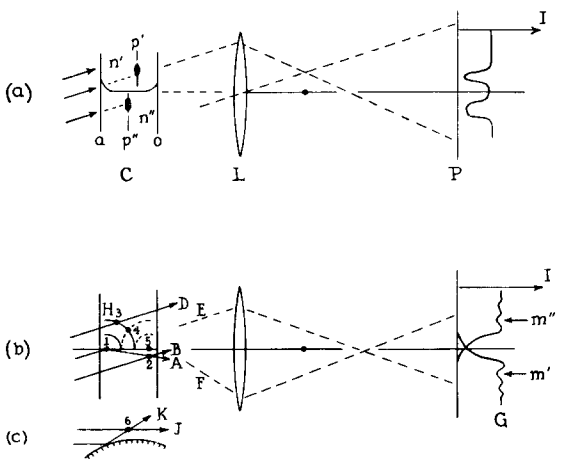

Fig. 8. Schematic intensity distributions resulting from reflection, interference, and diffraction phenomena associated with imaging a deep interface. C cell containing interface between two transparent fluids of indices of refraction n′ and n″. L lens focusing p′ and p″ at P. Dot on optical axis represents focal point of L. I qualitative intensity distribution at P. (a) Effect of contact of interface with cell walls "o", front and "a", back. (b) Effect of interface causing reflection and source of secondary wavelets. A Totally reflected ray. H Huygens wavelet from reflection point 1. B, D direct rays. E, F Diffracted light directions, even with normal illumination on cell. G Flanking fringe intensity pattern at P. m′ and m″ corresponding fringes on either side of the geometrical location of the interface. (c) Interference with a reflecting cylinder. J direct ray. K reflected ray.

References p. 431.

The flanking fringes appear to be due to the flat portion of the interface between the upper and lower quartz windows. Fig. 8(b) shows the effect on such an object of finite depth, in which the discontinuity between the two media causes both reflection of grazing light A at ①, and sources of Huygen's secondary wavelets, H. Interference could conceivably occur (a) at ② between the direct ray B and the reflected ray A, (b) at ③ between the direct ray D and a secondary wavelet ray from ①, or (c) at ④ between two secondary wavelets from ① and ⑤, for example. It seems likely that reflection does occur, and gives rise at least to the deflection of Fig. 4 interior to the meniscus pattern. Reversal of the apparent deflection would occur with the reversal of the off-axis displacement of the light source. Experimentally, the spacing between fringes increases as the focal plane is moved from the back face toward the front face of the cell, and is unchanged if the main light source image is blanked out.

It was hoped that one of the bands in the intensity patterns of (*a*) or (*b*) would correspond to the infinitely thin shadow attributed to the infinite gradient of the refraction index at the interface. None do so, however, apparently because instead, the "infinite gradient" causes a diffraction-like effect. In addition, the contacts of the interface with the front and back windows cause a shadow effect which is superimposed on the "infinite-gradient" position. Thus the main shadow is much too wide and complex to be caused simply by an "infinite gradient" and resort to the bisector of corresponding flanking fringes as the geometrical location of the meniscus is proposed. Theoretical support for this choice may exist in the literature. However, the author found only a series of papers describing fringes near a perfectly reflecting cylinder of large radius[14,15,16]. The optical arrangement is shown in Fig. 8c. The fringes which have been published appear similar to those from one side of the meniscus, or from the mercury-mirror cell (Fig. 5). There is no double central shadow, probably because the cylinder has no contact with windows as does the centrifuge meniscus. The variation of spacing with the focus is qualitatively the same as depicted in Fig. 5 col. (a). BRUSH[14] proposes that the fringes are due to a superposition of diffraction patterns which are not in register, and due to considering the cylindrical surface as a great many parallel diffracting elements. This is the mechanism mentioned in (c) above. However, BASU[15], points out that BRUSH neglected the part played by the light *K* regularly reflected from the surface which interferes with the direct rays *J* at ⑥. In fact, he, and subsequently CHINMAYAM[16], derive expressions for this effect alone which quantitatively describe the intensity and spacing of the fringes. Thus in this case, the effects (a) and (b) above appear to be dominant. With the (plane) meniscus, though, the blocking of the direct light does not alter the flanking fringes, which apparently rules out (a) and (b). The corresponding experiment with the cylinder was not reported. Extension of the reflecting cylinder theory to the centrifuge meniscus will have to consider fringes on both sides of the geometrical shadow and the role of light penetrating the interface as well as the role of the contact at the windows.

The explanation for the interference fringes which appear in the region of the meniscus central shadow when the main light source image is blocked can be patterned after the one proposed by TEMPLE[17] for interference fringes made to appear in a schlieren system in general when the light-source image is similarly blocked by a fine wire. He states that the presence of the object in the illumination system of light source to light-source image gives rise normally to diffracted light which passes through other points than the apparent light-source image. In Fig. 8(b), *E* and *F*

References p. 431.

do not pass through focal point indicated by dot. If part of this entire bundle of light through the camera lens is cut off or is otherwise modified, the balance is destroyed in the interference process by which the image, at the photographic plate, of the object is formed. As a result this image is altered, especially by the appearance of fringes. Because of the variability of these additional fine-structure bands, they have not been exploited here for information as to the precise position of the interface.

This study yields no information on the proper plane in the cell which should be set in focus on the screen[18]. Since the camera lens and plate remain fixed, camera magnification also remains constant even though the effective focal plane may vary (a) from drive to drive because of variable rotor shaft length, or variations in the shock mounting, (b) owing to a lift of the rotor with speed, (c) because of different refraction indices of solutions, or (d) because of different size centerpieces. Even so, this variation is not critical in the qualitative or quantitative interpretation of schlieren patterns, but may have to be considered carefully in interferometric patterns[18,19]. It should be noted that by using the bisector of flanking fringes, the observed meniscus level is determined without the exact plane of focus being known. A complication arises in interference optics for a different reason. If the light source is oriented 90° to that used in schlieren optics, it has parts which are off-axis and hence yields a very broad meniscus pattern (several mm on the plate). Similarly, with the absorption optics, a wide slit is used, and the meniscus is again broad and complex. It is thus recommended that in these two cases, the true meniscus position be determined with the light source in normal schlieren position.

The δ *vs.* r plots are used in this paper to give information of the location of r_a. However, in the practical application of the ARCHIBALD principle, it appears possible to consider r_a as known and thus determine some other independent information from the experiment, *e.g.* heterogeneity. It is true that as longer and longer times are used, the δ *vs.* r plot becomes horizontal, and there is no error in δ_a for an error in r_a. However, these studies indicate that if a $\pm$ 1 % error contributed by radial measurements alone is permissible in the molecular weight, then very short times can be used in which $\Delta M/\Delta r \lesssim 10\,\%/0.1$ mm, since the bisector method yields r_a to $\pm$ 0.01 mm on the plate.

ACKNOWLEDGEMENTS

The author is grateful for the opportunity to discuss the note by Dr. PING YAO CHENG prior to publication, to Dr. WALTER L. HUGHES for the use of the Spinco Interference Optics Assembly, and to Mr. GEORGE FLATTER and Mr. THEODORE SALATA, Spinco Field Service Engineers, for valuable advice and discussions pertinent to modification of the ultracentrifuge and its alignment.

SUMMARY

1. Ribonuclease sedimenting in 6 *M* urea is used to show that the apparent molecular weight calculated by the ARCHIBALD principle at times less than 3 h at any speed varies about 10 % per 0.1 mm error in location of the meniscus on the photographic plate.

2. The main shadow conventionally chosen as the meniscus, instead of being due to the infinite index of refraction gradient casting light out of the system, is probably due to the contact of the meniscus with the top and bottom quartz windows. Since both points cannot be in focus simultaneously, the appearance of their shadows (denoted as the "central shadow") is extremely de-

References p. 143.

pendent upon optical adjustments, especially the position of the light source relative to the optical axis and the camera focus. The central shadow can appear double for off-axis illumination and is a function both of speed and optical properties with pressure of the fluids forming the interface. It is not used in precision location of the meniscus.

3. A double system of diffraction-like bands in the meniscus region is independent of the position of the light source, speed, or the nature of the fluids forming the interface. The bisector between corresponding bands in each half of the double pattern is independent of camera focus, and is chosen to be the location of the interface. The double set of bands are denoted as "flanking fringes" and are probably due to the flat portion of the interface between the windows. The interference causing these fringes may be due to a complex interaction of totally reflecting light and secondary wavelets from the discontinuity.

4. In the absence of detailed optical theory of the fine-structure, the location to $\pm$ 0.01 mm on the plate of the flanking fringe bisector was indirectly verified as the top of the solution column by test of ribonuclease in acetate buffer. The common intersection of $(\partial c/\partial r)/rc$ curves occurred at the location of the bisector.

5. Modification of the Spinco Model E ultracentrifuge to enable direct viewing of the image in the plane of the photographic emulsion is described.

6. Special cells are described which are useful in instrumentation studies. In particular, a mirror quartz facilitates alignment of the light source onto the optical axis so that the central shadow approximates the position of the flanking fringe bisector.

7. A channel mask is described which screens out the meniscus from the solvent side when a double sector centerpiece cell is used. This enables simplification of the complex meniscus region in a separate reacceleration of the cell at the completion of a molecular weight experiment.

REFERENCES

1 R. TRAUTMAN, *J. Phys. Chem.*, 60 (1956) 1211.
2 W. J. ARCHIBALD, *J. Phys. Chem.*, 51 (1947) 1204.
3 P.-Y. CHENG, *J. Phys. Chem.*, 61 (1957) 695.
4 T. SVEDBERG AND K. O. PEDERSEN, *The Ultracentrifuge*, Clarendon Press, Oxford, 1940.
5 V. N. SCHUMAKER AND H. K. SCHACHMAN, *Biochim. Biophys. Acta*, 23 (1957) 628.
6 R. A. BROWN, D. KRITCHEVSKY AND M. DAVIES, *J. Am. Chem. Soc.*, 76 (1954) 3342.
7 A. GINSBURG, P. APPEL AND H. K. SCHACHMAN, *Arch. Biochem. Biophys.*, 65 (1956) 545.
8 G. KEGELES, S. M. KLAINER AND W. J. SALEM, *J. Phys. Chem.*, 61 (1957) 1286.
9 C. H. HIRS, W. H. STEIN AND S. MOORE, *J. Biol. Chem.*, 211 (1954) 941.
10 L. J. MILCH, *Lab. Invest.*, 2 (1953) 441.
11 H. SVENSSON, *Arkiv. Kemi, Mineral. Geol.*, 22A, No. 10 (1948).
12 R. TRAUTMAN AND V. W. BURNS, *Biochim. Biophys. Acta*, 14 (1954) 26.
13 J. J. BIKERMAN, *Surface Chemistry for Industrial Research*, Academic Press., Inc. New York, 1948.
14 C. F. BRUSH, *Proc. Am. Phil. Soc.*, 52 (1913) 276.
15 N. BASU, *Phil. Mag.*, 35 (1918) 79.
16 T. K. CHINMAYAM *Phil. Mag.*, 37 (1919) 9.
17 E. B. TEMPLE, *J. Opt. Soc. Amer.*, 47 (1957) 91.
18 H. SVENSSON, *Optica Acta, (Paris)*, 1 (1954) 25.
19 L. G. LONGSWORTH, *J. Phys. Chem.*, 61 (1957) 244.

Received October 18th, 1957